View metadata, citation and similar papers at core.ac.uk

brought to you by CORE

provided by Elsevier - Publisher Connector

Available online at www.sciencedirect.com

ScienceDirect

Progress in Natural Science: Materials International 24 (2014) 191–198

Progress in Natural Science Materials International

www.elsevier.com/locate/pnsmi
www.sciencedirect.com

Original Research

Activated carbon derived from rice husk by NaOH activation and its application in supercapacitor

Khu Le Van*, Thu Thuy Luong Thi

Physical Chemistry Department, Hanoi University of Education, Hanoi 1000, Vietnam

Received 21 October 2013; accepted 13 May 2014
Available online 10 June 2014

Abstract

Four activated carbon (AC) samples prepared from rice husk under different activation temperatures have been characterized by N_2 adsorption–desorption isotherms, thermogravimetric analysis (TGA–DTA), Fourier transform infrared spectroscopy (FTIR) and scanning electron microscopy (SEM). The specific surface area of AC sample reached 2681 $m^2\,g^{-1}$ under activation temperature of 800 °C. The AC samples were then tested as electrode material; the specific capacitance of the as-prepared activated carbon electrode was found to be 172.3 $F\,g^{-1}$ using cyclic voltammetry at a scan rate of 5 $mV\,s^{-1}$ and 198.4 $F\,g^{-1}$ at current density 1000 $mA\,g^{-1}$ in the charge/discharge mode.
© 2014 Chinese Materials Research Society. Production and hosting by Elsevier B.V. All rights reserved.

Keywords: Rice husk; Activated carbon; Supercapacitor; Surface area; Micropore

1. Introduction

Vietnam became the world's top rice exporter and exported 5.949 million tons of rice in the year 2012. Normally, rice husk is treated as waste and disposed at power plant sites, and leads to a serious environmental problem. Therefore, it is important to make full use of the husk. Recently, rice husk is used as precursors to produce activated carbon (AC) [1], zeolite [2,3], silica [4,5], concrete [6], etc. With porous structure, high surface area and low cost, AC has attracted considerable attention and has been widely used as catalyst carriers (catalytic support), adsorbent to adsorb metal ions and organic molecules or as electrode materials for batteries and capacitors [7], etc.

Supercapacitors are promising energy storage devices due to their high power density, high energy density and long cycle life. On the basis of the charge storage mechanism, supercapacitors are basically classified into three categories: electric double layer capacitors (electrostatic charge accumulation at the electrode–electrolyte interface), pseudocapacitors (fast and reversible redox processes at the electroactive material surface) and hybrid capacitors (the electric double layer capacitance and the pseudocapacitance) [8]. In the case of AC, the energy is stored in the electric double layer, which occurred at the porous carbon electrode/electrolyte interface [9]. In order to obtain a reasonable energy density, activated carbon must have high specific surface area to ensure high specific capacitance value, low resistivity and micro-texture well adapted in order to allow good electrolyte accessibility into the inner surface of the electrode [10]. Moreover, specific capacitance was not linearly proportional to the surface area, but strongly depended on the pore structure.

The aim of this work is to prepare a low-cost, high specific surface area activated carbon with microporous and mesoporous ranges using rice husk as the raw material. The effects of activation temperature on the specific surface area, pore structure, morphology and thermal stability of the AC samples have been examined. The AC samples were proved to be

*Corresponding author. Tel.: +84 4 38330842.
E-mail address: lvkhu@yahoo.fr (K. Le Van).
Peer review under responsibility of Chinese Materials Research Society.

Production and hosting by Elsevier

http://dx.doi.org/10.1016/j.pnsc.2014.05.012
1002-0071/© 2014 Chinese Materials Research Society. Production and hosting by Elsevier B.V. All rights reserved.

excellent electrode material for supercapacitor, hence solve the disposal and pollution problems of rice husk.

2. Experimental

2.1. Preparation of activated carbon

Activated carbons (ACs) were prepared from rice husk as following procedures: firstly, the rice husks (supplied by the Vinh Yen Region of Vietnam) were washed with water to remove dirt and other contaminants, oven-dried at 110 °C for 12 h then grounded and sieved to fractions with average particle size of 1.0 mm. Secondly, the prepared husks were carbonized at 400 °C under nitrogen flow (300 mL min^{-1}) for 90 min. The resulting samples were impregnated with NaOH (weight ratio 1/3) and dried at 120 °C for 12 h. Then, the preparative process was followed by heating at 400 °C for 20 min under nitrogen atmosphere at a flow rate of 300 mL min^{-1}; thereafter the temperature was raised to the predetermined temperatures (650–800 °C) at a heating rate of 10 °C and maintained at the final temperature for 60 min to activate the obtained material. Finally, the activated product was grounded, neutralized by 0.1 M HCl solution and washed several times with hot distilled water to a constant pH (6.6–7.0). The washed activated carbon samples were dried under vacuum at 120 °C for 24 h and stored in a desiccator. The final samples were labeled as RHN-650, RHN-700, RHN-750 and RHN-800 according to activated temperatures 650, 700, 750 and 800 °C, respectively.

2.2. Characterization of activated carbons

The surface functional groups of AC samples (ACs) were identified by Fourier transform infrared spectroscopy using an IR Prestige 21, Shimazu, operating in the range of 4000–500 cm^{-1} and employing the KBr pellet method. The surface acidity and basicity of the samples were determined by the Boehm method [11]. About 0.2 g of each AC sample was added to 25 mL of one of the four reactants of 0.1 M concentration: $NaHCO_3$, Na_2CO_3 NaOH and HCl. The mixtures were shaked for 48 h and then filtered to remove the carbon. The excess of base and acid was titrated with 0.1 M HCl solution and 0.1 M NaOH solution, respectively. The numbers of acidic sites were calculated under the assumption that NaOH neutralizes carboxyl, phenolic and lactonic groups; Na_2CO_3-carboxyl and lactonic groups; and $NaHCO_3$ only carboxyl groups. The number of surface basic sites was calculated from the amount of hydrochloric acid which reacted with the ACs.

The morphology of the AC was obtained with a field emission scanning electron microscope (S4800-Hitachi) coupled with the EDX analyzer.

Thermogravimetric analysis was performed in a Thermogravimetric Analyzer (DTG-60H, Shimazu). The AC samples were heated in pure air (flow rate 50 mL min^{-1}) at 10 °C min^{-1}, and within the temperature range 80–650 °C. Measurements were performed using calcined alumina as reference material.

The textural characterization of the ACs was based on the N_2 adsorption isotherms, determined at 77 K using a Micromeritics model Tri Star 3020 analyzer. The AC samples were outgassed for 24 h at 573 K to remove any moisture or adsorbed contaminants that may have been presented on their surface. The specific surface area (S_{BET}) was calculated by applying the BET equation to the adsorption data [12]. The microporous surface area (S_{mi}) and external surface area (S_{ex}), as well as the micropore volume (V_{mi}) were evaluated by the *t*-plot method [13]. The mesopore volume (V_{me}) was estimated by the Barrett–Joyner–Halenda (BJH) method [14]. The total pore volume (V_{tot}) was evaluated by the sum of microporous and mesoporous volumes. The pore size distribution of AC samples was calculated using density functional theory (DFT) [15] assuming that the pores of the sample have slit shapes.

2.3. Electrode preparation and electrochemical measurements

The working electrodes were constituted by an aluminum foil current collector and the active material. Composite of the active material was prepared by mixing the ACs, carbon black, and polytetrafluoroethylene (PTFE) with a ratio of 80/10/10 (by weight) in ethanol. The mixture was then heated at 60–80 °C to partially evaporate the solvent. The mixed slurry was laminated on each side of current collector and dried in an oven at 120 °C for 15 h. The resulting Al foil was pressed under 20 MPa and cut to a geometric surface area of about 1 cm^2.

Electrochemical measurements were carried out by an electrochemical work station (Autolab 302N) using a three-electrode system in 0.5 M K_2SO_4 electrolyte. A platinum sheet electrode and a saturated calomel electrode (SCE) served as the counter and reference electrode, respectively. Cyclic voltammetry (CV) measurements were conducted with a potential window from −1.0 to 0.0 V vs. SCE at different sweep rates ranging from 2 to 50 mV s^{-1}. Galvanostatic cycling with potential limitation (GCPL) test was carried out at a constant current density in the range from 500 to 2000 mA g^{-1}.

3. Results and discussion

3.1. Characterization of activated carbon

The qualitative characterization of surface functional groups of AC samples was performed by the FTIR technique. The results illustrated in Fig. 1 show that all the FTIR spectra have similar shapes with most of the bands located on the same wave number range. The band at 3425 cm^{-1} can be assigned to O–H stretching of hydroxyl groups or adsorbed water [16]. The bands at 2924 and 1393 cm^{-1} are attributed to C–H stretching of aliphatic carbon or due to CH_2 of CH_3 deformation. The band at 2858 cm^{-1} indicates the vibration of CH_3–O group. The band appearing at 1627 cm^{-1} corresponds to the C=O vibration of lactonic, carboxyl or anhydride groups [17]. The bands around 1545 and 1096 cm^{-1} are assigned to ring

vibration in a large aromatic skeleton generally found in carbonaceous material, such as activated carbon [18]. The region between 700 and 1200 cm^{-1} contains various bands related to aromatic, out of plane C–H bending with different degrees of substitution [19]. There are no SiO_2 absorption peaks at 1101, 944, 789 and 470 cm^{-1} [5]; therefore the FTIR declares that the AC samples are activated carbons without silica.

The distribution of chemical surface groups for ACs sample under study, determined by the Boehm titration technique, is presented in Table 1. The total acidic groups decrease gradually with increasing activation temperature. Whereas these phenomena have not been observed for the total basic groups. This result can be explained by the decomposition of the surface functional group at different activation temperatures. The acidic groups (carboxylic, lactonic, and phenolic) are decomposed at 100–650 °C, lower than that of basic groups (quinone, carbonyl, at 650–980 °C) [20]. Therefore the highest activation temperature leads to the lowest amount of acidic groups. Note that the sample RHN-800 with the highest activation temperature has larger amount of basic group, which is beneficial for capacitance promotion [9,21].

Scanning electron micrographs of AC samples were shown in Fig. 2. It can be seen from the pictures that all the AC samples exist in the form of spherical shaped particles with a size of about 10 nm that aggregated together to form pieces with different sizes. The size of the pieces increases slightly with increasing activation temperature. All the AC samples have porous structure with cracks and crevices.

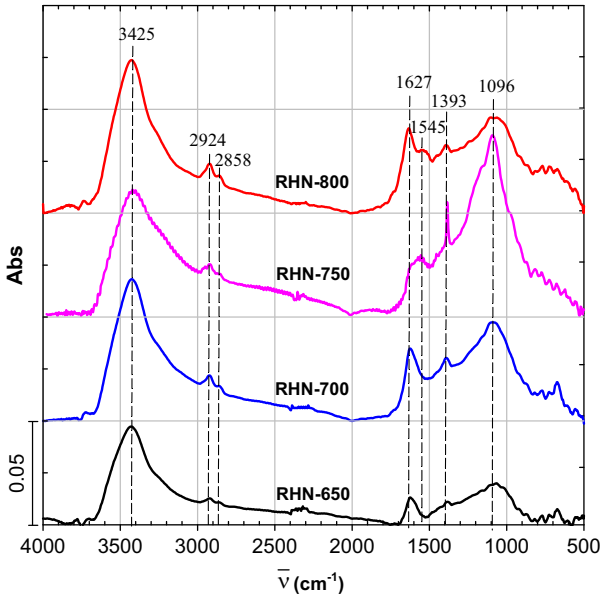

Fig. 1. FTIR spectra of the AC samples.

The thermal behaviors (TGA and DTA) of the ACs in the range of temperature 80–650 °C were shown in Fig. 3. The first step of weight loss was observed up to 350 °C, corresponding to the decomposition of carboxyl and lactonic groups present on the surface of the ACs [20]. According to Table 2, the weight loss in the first step descends with the increase of activation temperature. This result is in agreement and consolidate with the results obtained by the Boehm titration method which is presented in the previous paragraph. The mass of the AC samples drastically decreases in the range of 350–620 °C and accompanied by a large exothermic peak at about 550 °C on the DTA curves, corresponding to the oxidation of the carbon in the specimen. No significant weight loss is observed after 620 °C and the total weight loss for all AC samples exceeds 93% which shows that AC samples contain only organic compounds. The elemental analysis of RHN-800 sample was detected by EDX measurement; the relative composition is 83.04% of carbon and 16.96% of oxygen (Fig. 4). There is no other element observed in the EDX spectrum, which is in agreement with FTIR and TGA results. This is due to the use of NaOH as an activation agent; NaOH reacts with silica to form sodium silicate that is soluble in water and is removed by the water washing process [22].

Nitrogen adsorption–desorption isotherms at 77 K for ACs elaborated from rice husk in this study are shown in Fig. 5. All the isotherms belong to a mixed type in the IUPAC classification, type I at low relative pressures (p/p^0) and type IV at intermediate and high relative pressures [23,24]. There is an important uptake at low relative pressures, characteristic of microporous materials. However, the knee of the isotherms is wide, no clear plateau is attained and a certain hysteresis slope can be observed at intermediate and high relative pressures, indicating the presence of large micropores and mesopores. It can also be seen that RHN-800 presents the widest hysteresis which indicates that the amount of mesopores in this sample is the highest among others.

Physical properties of ACs obtained from N_2 adsorption are listed in Table 3. As can be seen from Table 3, the ACs exhibit a developed BET surface area and a high pore volume. The surface area varies from 2482 to 2681 $m^2\,g^{-1}$ and pore volume varies from 1.2929 to 1.4016 $cm^3\ g^{-1}$. The BET

Table 1
Acidic and basic surface characteristics of the activated carbons.

Sample	Groups			Total acidity (meq g^{-1})	Total basicity (meq g^{-1})
	Carboxylic (meq g^{-1})	Phenolic (meq g^{-1})	Lactonic (meq g^{-1})		
RHN-650	0.53	0.59	0.47	1.60	0.48
RHN-700	0.45	0.44	0.43	1.32	0.43
RHN-750	0.36	0.40	0.39	1.16	0.45
RHN-800	0.26	0.34	0.34	0.94	1.08

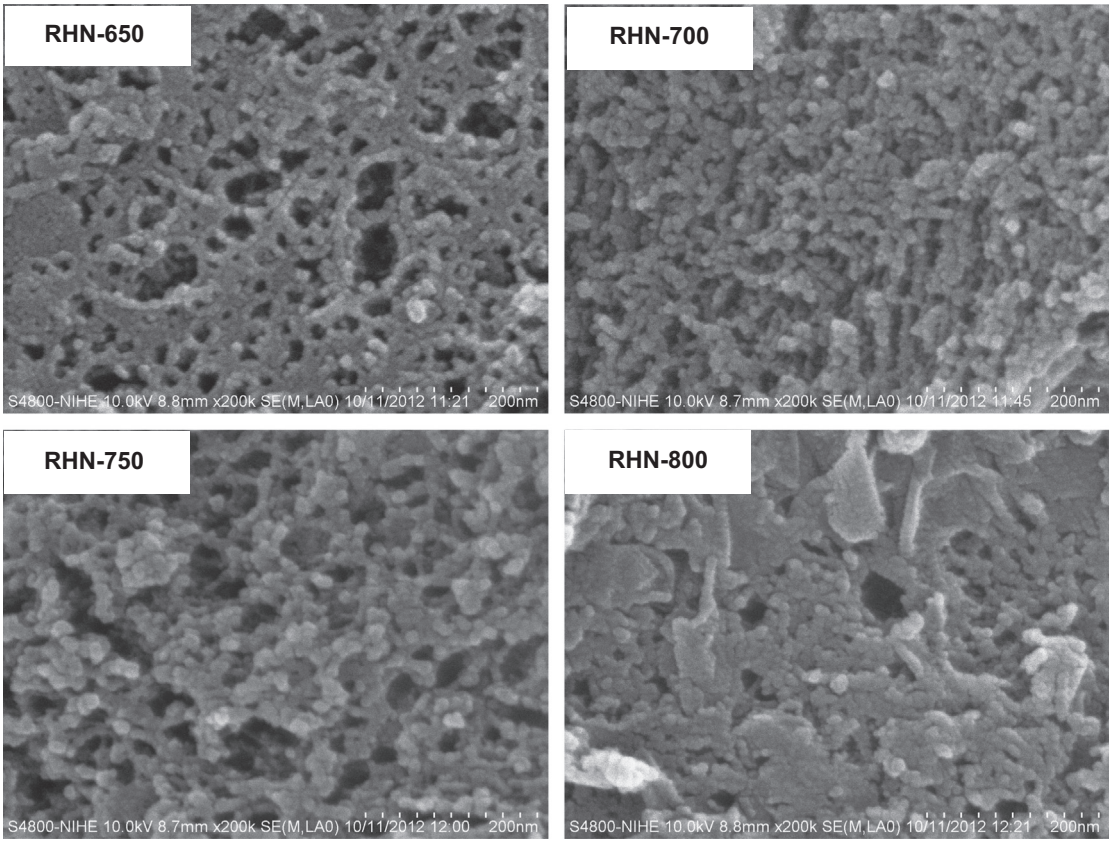

Fig. 2. SEM pictures of AC samples.

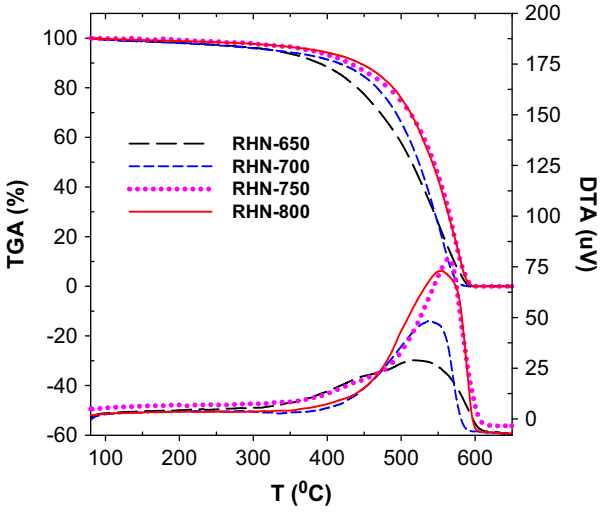

Fig. 3. TGA and DTA profiles of the activated carbons.

surface area slightly increases with activation temperature and mostly contributed by micropore area. The increase in surface area can be attributed to the release of volatile components after heat treatment. The AC sample activated at 800 °C (RHN-800) presented the highest BET surface area (2681 m^2/g).

Pore size distributions (PSDs) of the AC samples calculated using the DFT software are illustrated in Fig. 6. The obtained PSDs indicate that pore width of all the AC samples is less than 10 nm; therefore, Fig. 6 only shows the PSDs in the size range of 0.8–10 nm. It can be noticed that all the ACs have the appreciable amount of micropores and small amount of mesopores. The mesopore amount slightly decreases in the order: RHN-800 > RHN-750 ≈ RHN-700 > RHN-650. Besides, only RHN-800 and RHN-700 possess some amount of mesopores of width above 4.0 nm, resulting in high mesopore volume. The obtained PSDs correspond well with and confirm the observation from N_2 adsorption–desorption at 77 K and the calculated values shown in Table 3.

Table 2
Weight loss of AC samples.

Sample	Weight loss in the temperature range (%)	
	80–350 (°C)	350–620 (°C)
RHN-650	6.25	93.75
RHN-700	5.75	94.25
RHN-750	3.60	96.40
RHN-800	3.56	96.44

3.2. Electrochemical feature of AC

Cyclic voltammogram (CV) of AC samples in 0.5 M K_2SO_4 at scan rates of 2, 10 and 30 mV s^{-1} is shown in Fig. 7. At the scan rate of 2 mV s^{-1}, all the AC samples show a symmetric

and quasi-rectangular shape profile typical of ideal electrochemical double layer capacitors, with very small humps attributed to pseudofaradaic redox reactions related to the surface functionalities of the materials [25]. RHN-650 presented the largest humps of all, which are due to the highest total acidic group of this sample (Table 1). With the increase of scan rate, the rectangular shape of voltammogram was distorted in order: RHN-800 < RHN-700 < RHN-650 ≈ RHN-750. This behavior could be explained by the textural characteristic of AC samples, RHN-800 and RHN-700 samples presented some amount of mesopores of width above 4.0 nm which facilitate to the diffusion of K^+ ion in the matrix of carbon.

Fig. 8 displays the CVs of RHN-800 electrode at different scan rates from 2 to 50 mV. As can be seen, the CVs which still remain rectangular shaped even at a scan rate up to 50 mV s^{-1} indicated a good capacitor behavior of the material even at high scan rate.

The gravimetric capacitance, C_{CV} (F g^{-1}), was calculated from CVs using the following equation:

$$C_{CV} = \frac{\sum |I| \Delta t}{2m\Delta V} \quad (1)$$

where $\sum |I| \Delta t$ is the area of the current (A) against time (s) curve, m is the mass of active material in the electrode (g), and ΔV is the potential window (V). The specific capacitances of AC samples electrodes at different scan rates were calculated due to Eq. (1) and are reported in Table 4. C_{CV} gravimetric capacitance decreases when the scan rate increases. Except for RHN-800, the C_{CV} value increases as the scan rate increases from 2 to 5 mV s^{-1}, and slightly decreases with further increase of scan rate. While the scan rate varied from 5 to

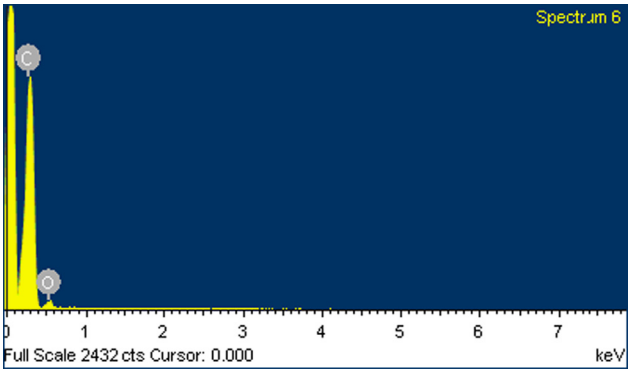

Fig. 4. EDX spectrum of RHN-800 sample.

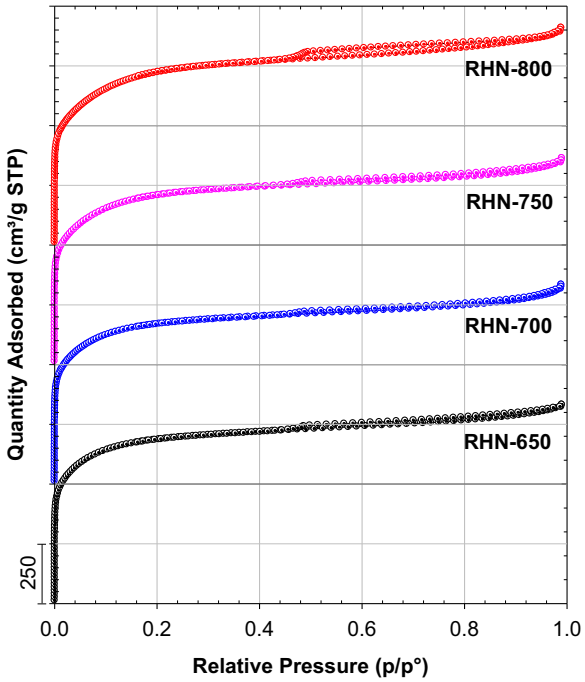

Fig. 5. N_2 adsorption–desorption isotherms at 77 K of ACs samples.

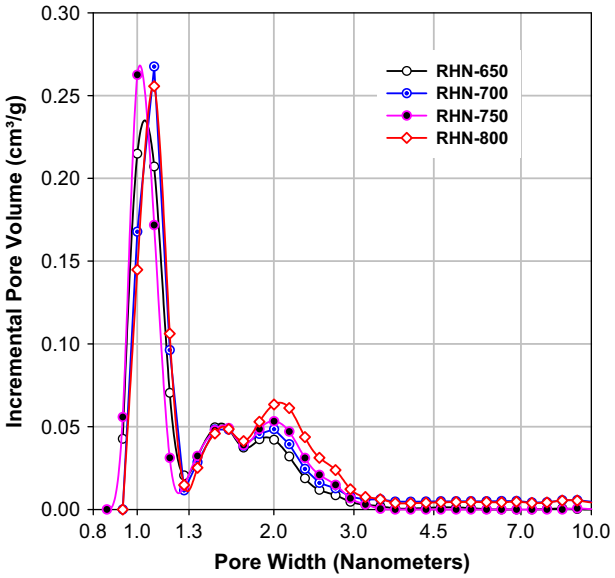

Fig. 6. Pore size distribution of AC samples prepared from rice husk.

Table 3
Physical properties deduced from N_2 adsorption at 77 K on ACs prepared from rice husk.

Samples	S_{BET} (m^2 g^{-1})	S_{mi} (m^2 g^{-1})	S_{mi}/S_{BET} (%)	S_{ex} (m^2 g^{-1})	V_{mi} (cm^3 g^{-1})	V_{me} (cm^3 g^{-1})	V_{tot} (cm^3 g^{-1})	V_{mi}/V_{tot} (%)
RHN-650	2520	2262	89.8	258	0.9637	0.3292	1.2929	74.5
RHN-700	2482	2238	90.2	244	0.9453	0.3476	1.2929	73.1
RHN-750	2617	2373	90.7	244	1.0081	0.3317	1.3398	75.2
RHN-800	2681	2376	88.6	305	1.0110	0.3906	1.4016	72.1

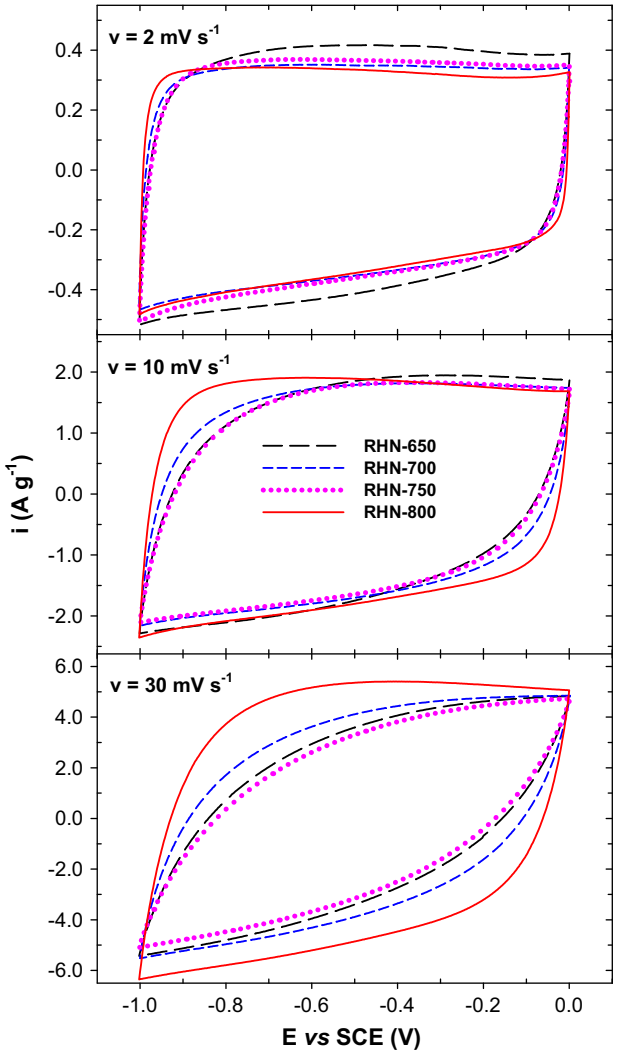

Fig. 7. CV curves of AC samples at different scan rates.

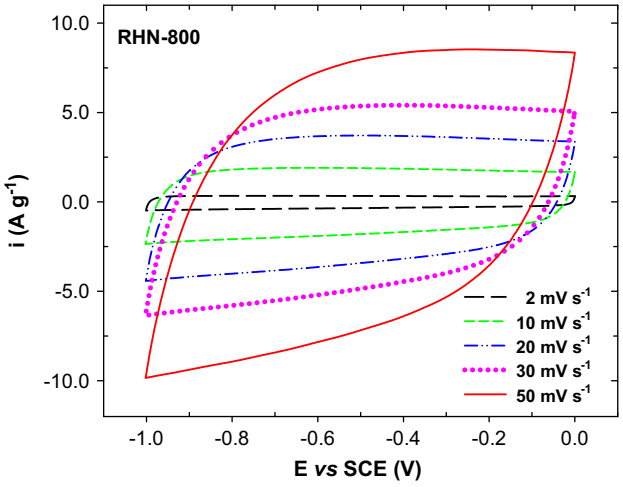

Fig. 8. CV curves of RHN-800 electrode at different scan rates.

50 mV s^{-1}, C_{CV} of all AC electrodes maintain the same order as RHN-800 > RHN-700 > RHN-650 > RHN-7500, demonstrated that the activation temperature in the preparative phase

Table 4
Gravimetric capacitance C_{CV} of the AC samples at different scan rates.

Scan rate (mV s^{-1})	C_{CV} (F g^{-1}) of samples			
	RHN-650	RHN-700	RHN-750	RHN-800
2	197.4	166.1	170.0	159.8
5	179.1	165.4	163.7	172.3
10	156.8	154.7	149.2	170.7
20	127.6	134.0	122.9	160.5
30	108.6	118.7	102.7	150.5
50	83.5	97.1	76.0	133.1

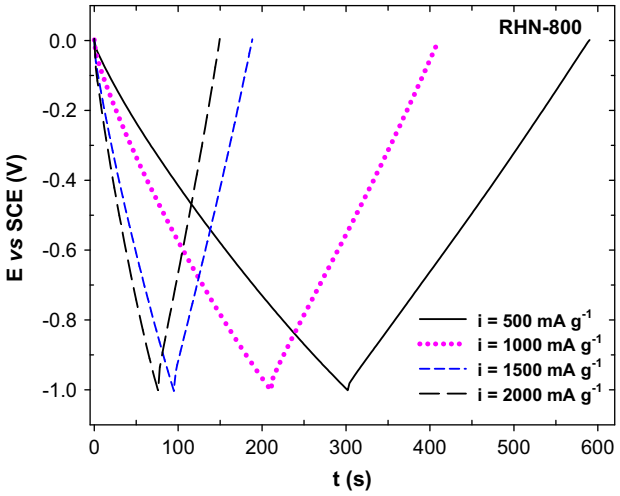

Fig. 9. Galvanostatic charge–discharge curves for RHN-800 at different current densities.

could play an important role in the electrochemical property of activated carbons. At the scan rate of 2 mV s^{-1}, the specific capacitance of RHN-800 electrode is 159.8 F g^{-1}, higher than that of PICACTIF activated carbon at the same scan rate [26], due to high specific surface area and high micropore volume of RHN-800 sample [26,27].

Galvanostatic cycling with potential limitation (GCPL) is a useful technique to identify charge/discharge cycling behavior of electrode material in electrochemical energy storage devices. Since RHN-800 exhibited the best behavior capacitor among the ACs under study in the CV test, the GCPL was performed with this sample. The chronopotentiograms of RHN-800 at current density loading between 500 and 2000 mA g^{-1} in a potential interval of −1.0 to 0.0 V vs. SCE are shown in Fig. 9. A sudden potential dropped at the beginning of the constant current discharge is designated as the IR drop, which is due to the resistance of electrolyte solution and the inner resistance of ion K^+ diffusion in porous carbon. However, all the curves present highly linear and symmetrical triangle indicating excellent capacitive behavior of the AC electrode even at high current density.

Table 5
Gravimetric capacitance C_{CP} of the RHN-800 sample at different current densities.

Discharge curent density (mA g^{-1})	500	1000	1500	2000
Gravimetric capacitance C_{CP} (F g^{-1})	144.3	198.4	142.2	142.1

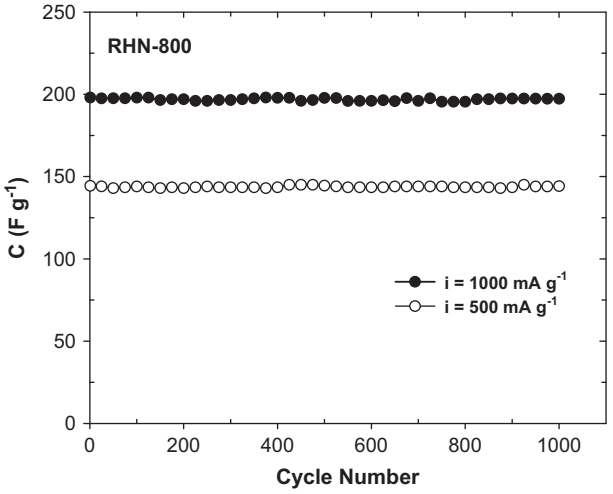

Fig. 10. C_{CP} of RHN-800 electrode at current density of 500 and 1000 mA g^{-1} for 1000 cycles.

The gravimetric capacitance from these measurements, C_{CP} (F g^{-1}), was obtained by the following equation:

$$C_{CP} = \frac{I_d \Delta t}{m \Delta V} \quad (2)$$

where I_d is the discharge current (A), m is the mass of active material in the electrode (g), Δt is the discharge time (s), and ΔV is the potential interval (V).

The specific capacitances of the RHN-800 sample at a current density loading between 500 and 2000 mA g^{-1} are listed in Table 5. As can be seen from Table 5, C_{CP} increases from 144 F g^{-1} and reaches the maximum value of 198 F g^{-1} when the current density increases from 500 mA g^{-1} to 1000 mA g^{-1}; with further increase of current density C_{CP} decreases and reaches the value of about 142.1 F g^{-1} at discharge current density of 2000 mA g^{-1}. The dependence of specific capacitance on current density could be explained as follows: the specific capacitance is a function of both the adsorption behavior of K^+ ion and the surface functional groups of AC. When the scan rate increases, the adsorption of K^+ ion decreases while the contribution of surface functional group increases; therefore, the trend of specific capacitance does not increase contemporaneously with the increase of current density.

Fig. 10 shows the charge/discharge cycling behavior of RHN-800 electrode at constant current density of 500 and 1000 mA g^{-1} for 1000 cycles. The specific capacitance values are stable over the 1000 cycles and about 99% of the initial specific capacitance is still retained, suggesting that the AC electrode has excellent charge/discharge ability.

4. Conclusion

Activated carbon from rice husk was successfully synthesized by chemical activation with NaOH as the activating agent at different activation temperatures in the range of 650–800^{0}C. The obtained materials were characterized and evaluated for potential application as supercapacitor electrode material. The AC samples have porous structure, variety surface functional groups and high specific surface area (S_{BET}=2482–2681 m^2 g^{-1}), which contains micropore and mesopore distributed mainly from 0.9 to 3.0 nm. High activation temperature resulted in high specific surface area (S_{BET}=2681 m^2 g^{-1}), high mesopore contribution (V_{me}=0.3906 cm^3 g^{-1}) and high total basic surface group (1.08 meq g^{-1}), which in turn improved gravimetric capacitance of AC when using as active material in supercapacitors. Specific capacitance of the as-prepared electrode reached 172.3 F g^{-1} at scan rate of 5 mV s^{-1} and 198.4 F g^{-1} at current density of 1000 mA g^{-1}. The latter was stable even after 1000 cycles of charge/discharge. So, AC obtained from rice husk by NaOH activation at 800 °C may be a suitable candidate for application as supercapacitor electrode material.

References

[1] T. Liou, S. Wu, J. Hazard. Mater. 171 (2009) 693–703.
[2] W. Panpa, S. Jinawath, Appl. Catal. B 90 (2009) 389–394.
[3] H.T. Jang, Y.K. Park, Y.S. Ko, J.Y. Leea, B. Margandan, Int. J. Greenh. Gas Control 3 (2009) 545–549.
[4] T. Liou, Carbon 42 (2004) 785–794.
[5] D. An, Y. Guo, B. Zou, Y. Zhu, Z. Wang, Biomass Bioenergy 35 (2011) 1227–1234.
[6] G. Gorhan, O. Simsek, Constr. Build. Mater. 40 (2013) 390–396.
[7] Y. Chen, Y. Zhu, Z. Wang, Y. Li, L. Wang, L. Ding, X. Gao, Y. Ma, Y. Guo, Adv. Colloid Interface Sci. 163 (2011) 39–52.
[8] P. Simon, Y. Gogotsl, Nat. Mater. 7 (2008) 845–854.
[9] Y. Guo, J. Qi, Y. Jiang, S. Yang, Z. Wang, H. Xu, Mater. Chem. Phys. 80 (2003) 704–709.
[10] J. Gamby, P.L. Taberna, P. Simon, J.F. Fauvarque, M. Chesneau, J. Power Sources 101 (2001) 109–116.
[11] H.P. Boehm, Carbon 40 (2002) 145–149.
[12] S. Brunauer, P.H. Emmett, E. Teller, J. Am. Chem. Soc. 60 (1938) 309–319.
[13] B.C. Lippens, J.H. de Boer, J. Catal. 4 (1965) 319–323.
[14] E.P. Barrett, L.G. Joyner, P.P. Halenda, J. Am. Chem. Soc. 73 (1951) 373–380.
[15] P.A. Webb, C. Orr, in: Analytical Methods in Fine Particle Technology, Micromeritics Instrument Corporation, Norcross, GA USA, 1997.
[16] Y. Guo, D.A. Rockstraw, Microporous Mesoporous Mater. 100 (2007) 12–19.
[17] L.J. Kennedy, J.J. Vijaya, G. Sekaran, Mater. Chem. Phys. 91 (2005) 471–476.
[18] R.C. Sun, J. Tomkinson, Sep. Purif. Technol. 24 (2001) 529–539.
[19] M. Mastalerz, R.M. Bustin, Fuel 74 (1995) 536–542.

[20] J.L. Figueiredo, M.F.R. Pereira, M.M.A. Freitas, J.J.M. Orfao, Carbon 37 (1999) 1379–1389.
[21] M.J. Bleda-Martinez, J.A. Macia-Agullo, D. Lozano-Castello, E. Morallon, D. Cazorla-Amoros, A. Linares-Solano, Carbon 43 (2005) 2677–2684.
[22] Y. Guo, S. Yang, K. Yu, J. Zhao, Z. Wang, H. Xu, Mater. Chem. Phys. 74 (2002) 320–323.
[23] K.S.W. Sing, D.H. Everett, R.A.W. Haul, L. Moscou, R.A. Pierotti, J. Rouquérol, T. Siemieniewska, Pure Appl. Chem. 57 (1985) 603–619.
[24] J. Rouquérol, D. Avnir, C.W. Fairbrige, D.H. Everett, J.H. Haynes, N. Pernicone, J.D.F. Ramsay, K.S.W. Sing, K.K. Unger, Pure Appl. Chem. 66 (1994) 1739–1758.
[25] K. Kinoshita, in: Carbon: Electrochemical and Physicochemical Properties, Wiley, New York, 1988.
[26] T. Brouse, P.L. Taberna, O. Crosnier, R. Dugas, P.l. Guillemet, Y. Scudeller, Y. Zhou, F. Favier, D. Belanger, P. Simon, J. Power Sources 173 (2007) 633–641.
[27] C. Zhang, R. Zhang, B. Xing, G. Chen, Y. Xie, W. Qiao, L. Zhang, X. Liang, L. Ling, New Carbon Mater. 25 (2010) 129–133.